Spectroscopic and electrochemical study of interactions between DNA and different salts of 1,4-dihydropyridine AV-153

Elina Leonova[1], Karlis Shvirksts[2], Vitalijs Borisovs[1,3], Edgars Smelovs[1], Jelizaveta Sokolovska[1], Egils Bisenieks[3], Gunars Duburs[3], Mara Grube[2] and Nikolajs Sjakste[1,3]

[1] Faculty of Medicine, University of Latvia, Riga, Latvia
[2] Institute of Microbiology and Biotechnology, University of Latvia, Riga, Latvia
[3] Latvian Institute of Organic Synthesis, Riga, Latvia

ABSTRACT

1,4-dihydropyridines (1,4-DHP) possess important biochemical and pharmacological properties, including antimutagenic and DNA-binding activity. The latter activity was first described for water-soluble 1,4-DHP with carboxylic group in position 4, the sodium salt of the 1,4-DHP derivative AV-153 among others. Some data show the modification of physicochemical properties and biological activities of organic compounds by metal ions that form the salts. We demonstrated the different affinity to DNA and DNA-protecting capacity of AV-153 salts, depending on the salt-forming ion (Na, K, Li, Rb, Ca, Mg). This study aimed to use different approaches to collate data on the DNA-binding mode of AV-153-Na and five other AV-153 salts. All the AV-153 salts in this study quenched the ethidium bromide and DNA complex fluorescence, which points to an intercalation binding mode. For some of them, the intercalation binding was confirmed using cyclic voltammetry and circular dichroism spectroscopy. It was shown that in vitro all AV-153 salts can interact with four DNA bases. The FTIR spectroscopy data showed the interaction of AV-153 salts with both DNA bases and phosphate groups. A preference for base interaction was observed as the AV-153 salts interacted mostly with G and C bases. However, the highest differences were detected in the spectral region assigned to phosphate groups, which might indicate either conformational changes of DNA molecule (B form to A or H form) or partial denaturation of the molecule. According to the UV/VIS spectroscopy data, the salts also interact with the human telomere repeat, both in guanine quadruplex (G4) and single-stranded form; Na and K salts manifested higher affinity to G4, Li and Rb –to single-stranded DNA.

Corresponding author
Nikolajs Sjakste,
Nikolajs.Sjakste@lu.lv

INTRODUCTION

Synthetic derivatives of 1,4-dihydropyridine (1,4-DHPs) possess various pharmacological properties, including antimutagenic and radioprotective effects. This study focused on a series of salts of the 1,4-DHP derivative AV-153. It was shown that AV-153-Na salt possesses antimutagenic activity, enhances the DNA repair, can protect DNA against genotoxic agents, and bind DNA (*Buraka et al., 2014*; *Leonova et al., 2018*; *Ryabokon et al., 2005*; *Ryabokon et al., 2008*; *Ryabokon et al., 2009*). The compound also stimulates cell growth, manifests anti-apoptotic activity, and possesses antioxidant properties (*Milkovic et al., 2018*). Different salts of the compound were recently synthesized and subjected to investigation. It is well-known that the formation of salt from a cyclic organic compound and metal causes a perturbation in the electronic system of the molecule. Alkali metals disturb the electronic structure of aromatic compounds. Metals also change the biological activity of organic compounds, including isonicotinates and nicotinic acid salts (*Koczoń et al., 2005*; *Lewandowski, Kalinowska & Lewandowska, 2005*), which are structurally close to 1,4-DHP. We showed in a recent study that metal ions modify the ability of the AV-153 to bind DNA and protect DNA in living cells against peroxynitrite or Tat-induced oxidative stress (*Leonova et al., 2019*). When administered to rats with experimental diabetes, AV-153-Na and AV-153-Ca produced different effects on the DNA repair-related and proteasomal genes (*Dišlere, 2019*). The metal ions remain complexed with the compound after dissociation, their modifying action on the AV-153 salt effects were produced in this dissociated state. The pKs of the salts ranged from pH 4.24 to 4.52, but all the experiments were performed at neutral pH (*Leonova et al., 2019*). These data encouraged us to conduct further studies of the interactions of AV-153 salts with DNA and proteins. We applied a set of physico-chemical methods to assess the impact of molecular modifications on the DNA binding mode. Interactions between the AV-153 salts and DNA were studied with cyclic voltammetry. The possible interaction mechanism was evaluated by means of EtBr displacement assay, circular dichroism, and infrared spectroscopy. We also tested the affinity of the AV-153 salts to telomeric repeats after taking the great interest in G-quadruplex-targeting drugs and recent reports on the possible application of the 1,4-DHP as G-quadruplex sensors into account (*Aghaei et al., 2017*).

MATERIALS AND METHODS

Chemicals

Different AV-153 salts (3,5-bis-ethoxycarbonyl-2,6-dimethyl-1,4- dihydropyridine-4-carboxylate) were synthesized in the Laboratory of Membrane Active Compounds at the Latvian Institute of Organic Synthesis. The structure of the AV-153 salts are shown in Fig. 1. The synthesis of the 2,6-dimethyl-3.5-bis(ethoxycarbonyl)-1,4-dihydroisonicotinic acid was performed as reported (*Duburs & Uldrikis, 1969*). Salts of monovalent metals (Na, Li, K, Rb) were prepared following the same procedure. At the final stage of the synthesis, the saturated water solution of the appropriate hydroxide was added to the hot 2,6-dimethyl-3,5-bis(ethoxycarbonyl)-1,4-dihydroisonicotinic acid solution in ethanol. Salts of divalent metals (Ca and Mg) were prepared by transmetallation reaction to the
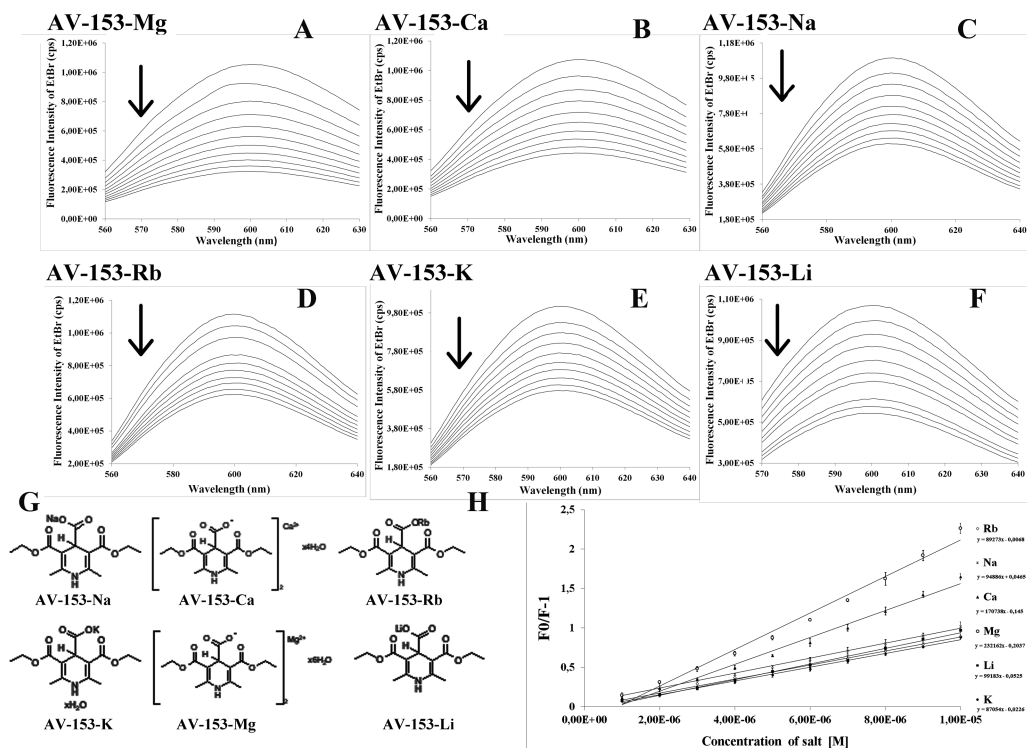
Figure 1 **Spectrofluorimetric ethidium bromide displacement assay.** (A–F) Changes in the spectra of EtBr-DNA complex induced by AV-153-Mg, AV-153-Ca, AV-153-Na, AV-153-Rb, AV-153-Rb, AV-153-Li, respectively. Six spectra out of 25 obtained are shown. (G) Formulas of the AV-153 salts. (H) Stern-Volmer plots.

sodium salt solution with the appropriate metal chloride in a water solution at room temperature. The obtained salts were dried in vacuo on phosphorus pentoxide and were fully characterized by ^{1}H NMR, LC/MS and elemental analysis. The purity of the salts determined by HPLC exceeded 95%. Tris base, ethidium bromide (EtBr), calf thymus DNA (ct-DNA), human serum albumin (HSA), Na$_2$EDTA, and inorganic salts were purchased from Sigma-Aldrich (Taufkirchen, Germany).

Cyclic voltammetry

For the voltammetric experiments we used an EcoChemie Autolab PGSTAT 302T potentiostat/galvanostat (Utrecht, The Netherlands) and the electrochemical software package Nova 2.0. We used a three-electrode system: a two mm-sized Pt disk working electrode, an Ag/AgCl reference electrode (3 M KCl) and a Pt wire counter electrode purchased from Metrohm Co (Herisau, Switzerland). Voltammograms of the 5 mM AV-153 salt solution in 0.1 M Tris–HCl (pH = 7.4) were first registered. After that, 10 μM of DNA was added and the measurements were repeated. This was repeated twice or more. Scan rate was 100 mV/s. Electrodes were washed with double-distilled water before each measurement. Experiments were performed at 25 °C. Samples were deoxygenized with oxygen-free nitrogen gas.

The binding constant was determined using the equation:

$$\log\left(\frac{1}{DNA}\right) = \log(K) + \log[I_{\text{free}}/(I_{\text{free}} - I_{\text{bond}})]$$

where K is the apparent binding constant; I_{free} is the peak current of free compound; and I_{bond} is the peak current of compound in the presence of DNA (*Feng, Li & Jiang, 1997*).

The number of binding sites was determined using the equation:

$$\frac{I - I_{DNA}}{I_{DNA}} = \frac{K[DNA]}{2s}$$

where I is the peak current of a compound in the absence of DNA; A, IDNA is the peak current of a compound in the presence of DNA; A, K is the binding constant of compound-DNA complex; [DNA] is the DNA concentration, mol/L; s is the size of the binding site (bp) (*Aslanoglu, 2006*). The number of electrons (n) was calculated using the equation:

$$E_p - \frac{E_p}{2} = 47.7 \text{ mV}/\alpha n$$

where Ep is the peak compound potential; mV; $Ep/2$ is the half-wave compound potential; mV, α –the assuming value = 0.539; n—number of electrons (*Wang et al., 2011*).

Fluorescence spectroscopic measurements

Spectrofluorimetry was performed using a Fluoromax-3 (Horiba JOBIN YVON, China).

To study the interaction of 1,4-DHP with the DNA-EtBr complex by means of the spectrofluorimetry, the calf thymus DNA (74.8 µM) and ethidium bromide (1.26 µM) were diluted in 5 mM Tris HCl; 50 mM NaCl at pH 7.4. Spectra were recorded in a 1-cm cuvette (2 ml) at room temperature. The AV-153 salts were added by 8 µl aliquots of the 2.5 mM solution. The solution was mixed thoroughly and kept for 5 min to equilibrate before the fluorescence measurement. Interactions of the tested compounds with DNA caused displacement of EtBr from the complex with DNA. The fluorescence was recorded at 109,600 nm using an indirect excitation wavelength of EtBr at 260 nm (*Geall & Blagbrough, 2000*). The linear Stern-Volmer equation, in which 1,4-DHPs were the quenchers, was applied for calculation of the quenching constants:

$$\frac{I_0}{I} = 1 + K_{sv}[Q]$$

Where I_0 and I represent the fluorescence intensities in the absence and presence of quenchers, respectively; K_{sv} is a linear Stern-Volmer constant; and Q is the quencher concentration. K_{sv} values were evaluated from the slope of the plot (*Geethanjali et al., 2015*). Linearity of the plots was tested by calculation of the correlation coefficient (*Gong & Zhu, 2013*; *Wahba, El-Enany & Belal, 2015*).

Circular dichroism spectroscopy

CD spectra were recorded on a Chirascan CS/3D spectrometer (Applied Photophysics, Surrey, UK), DNA and compound binding measurements were done in 10 mM HEPES buffer, and pH 7.4 in a quartz cell of 10 mm path-length at room temperature. The CD
spectra of ct-DNA and G4 structure were recorded in 220–320 nm range, and that of the HSA in a 200–260 nm range. The parameters for all spectra were as follows: scan rate (200 nm min^{-1}), averaging time (0.125 s), bandwidth (1 nm) and one recorded spectrum is the average of four scans. We carried out titrations in the DNA region by adding increasing amounts of AV-153 salts (10 μM at each step) to a 50 μM DNA solution. Titrations in the induced CD compound region were performed by adding DNA (62.5 μM at each step) to a 500 μM AV-153-Na solution.

UV/VIS spectroscopic measurements were applied for a study of the AV-153 salts interaction with bases (Sadeghi et al., 2016) and oligonucleotides corresponding to human telomere repeat sequence. The spectra were recorded with a Perkin Elmer Lambda 25 UV/VIS spectrophotometer. Spectra of a 25 μM solution of the tested compound in 50 mM NaCl and 5 mM Tris HCl at pH 7.4.were taken in a one cm quartz cell (2 ml) in the absence of bases and after adding 10 μM of bases.

In the case of human telomere repeats the titration was performed in 10 mM sodium phosphate buffer, 0.3 mM EDTA, 100 mM NaCl, pH 7.2, 50 nM of oligonucleotide were added each time.

The binding constants were calculated using the formula:

$$\frac{1}{A_0 - A} = \frac{1}{A_0} + \frac{1}{K \times A_0 \times c_{DNA}}$$

Where A_0 is absorption of the free substance; A is absorption in the presence of DNA; and C_{DNA} is the DNA concentration (*Buraka et al., 2014*).

Fourier transform infrared (FTIR) spectroscopy

For the FTIR analyses AV-153-Li and AV-153-K were dissolved in distilled water (H2O), but AV-153-Ca, AV153-Mg, and AV-153-Rb were dissolved in dimethyl sulfoxide (DMSO). Aliquots containing from 5 to 10 μL of 7.5 mM DNA solutions, AV-153 salts or a mixture of DNA and the salts in a ratio of 1:5 were dried at T<50 °C on a 384-well silicone plate. The FTIR absorption spectra were recorded on a VERTEX 70 coupled with an HTS-XT microplate reader extension (BRUKER, Germany) over a 4,000–6,000 cm^{-1} range with a four cm^{-1} resolution, with 64 scans co-added. The baseline was corrected using the rubber band method, and CO$_2$ bands were excluded. Spectra with absorption limits between 0.25 and 0.80 were used for data analyses in accordance with the Lambert-Bouger-Beer law, that is, the concentration of a component should be proportional to the intensity of the absorption band. The data were processed using OPUS 6.5 software.

Interaction with single-stranded and guanine quadruplex forming oligonucleotides

Oligonucleotide corresponding to human telomere repeat (5′-AGGGTTAGGG TTAGGGTTAGGG-3′) was ordered in Metabion. To induce the formation of the antiparallel G4, the oligonucleotide was heated at 90° and allowed to slowly cool down for 1 h at room temperature and then for 3 d in 10 mM sodium phosphate buffer, 0.3 mM EDTA, 100 mM NaCl, pH 7.2 at +4 °C in a 10 mm path-length quartz cell at room temperature. The G4 formation was checked with circular dichroism spectroscopy (CD).

To observe the interactions of AV-153 salts with the oligos, 5 μM of the oligonucleotide were titrated in 10 mM sodium phosphate buffer, 0.3 mM EDTA, 100 mM NaCl, pH 7.2 with 10 μM of AV-153 salt at each step, CD spectra were recorded after each stabilization of the solution (5 min) in a 220–320 nm range at room temperature. In a parallel binding of the oligo in G4 and single-stranded form (before the 3rd day of incubation in the presence of salt) was assayed with UV/VIS spectroscopy, as described above. A solution of AV-153 salts of monovalent metals (25 μM) in the buffer was titrated with either G4 or single-strand oligonucleotides, 50 nM each time.

Statistics

All measurements were performed in triplicate. Numerical data are presented as mean ± S.E.M.

RESULTS

Electrochemical study of the interactions between AV-53 salts and DNA

Cyclic voltammograms of 5 mM AV-153-K in the absence and presence of various DNA concentrations in 0.1 M Tris–HCl buffer, pH = 7.4 are shown in Fig. 2. The peak potential shifted to a more positive value (0.018 V) in the presence of DNA. A slight increase in the peak current upon the addition of increasing concentrations of DNA was also observed. The compound exhibited a single well defined anodic peak, which corresponds to the oxidation of the dihydropyridine ring (*Augustyniak et al., 2010*). No peak was observed in a reverse scan, indicating that the oxidation of the compound is an irreversible process. The peak current (Ip) of the oxidation wave AV-153-K was proportional to the square root of the scan ($v^{1/2}$). The cyclic voltammograms of other AV-153 salts were similar (not shown). The differences in the binding constants of the AV-153 salts were calculated using cyclic voltammetry data followed the same trend as affinity to DNA formerly determined spectrofluorimetrically (*Leonova et al., 2019*) (see Table 1).

Fluorescent intercalator displacement assay

To assess the mode of the DNA interaction with the AV-153 salts we have performed a fluorescent intercalator displacement assay. The method is based on the quenching of the enhanced fluorescence of the DNA-EtBr complex by a second ligand (*Ghosh et al., 2010*). As presented in Fig. 1A, all AV-153 salts quenched the EtBr fluorescence up to 70%, indicating that the compounds competed with EtBr for DNA intercalation sites. The Stern-Volmer quenching constant calculations indicated that Ca and Mg salts displaced the EtBr from intercalation sites more intensively than Na, Li and K salts, and Rb salt produced the weakest effect. (Fig. 1B, Table 2).

Circular dichroism

Circular dichroism spectra of ct-DNA in the presence of increasing concentrations of AV-153-Rb and AV-153-Ca are shown in Fig. 3. The DNA manifested a negative band at 245 nm due to helicity and a positive band at 270 nm because of base stacking which is characteristic of the B form of DNA. Adding AV-153 salts to DNA increased the negative
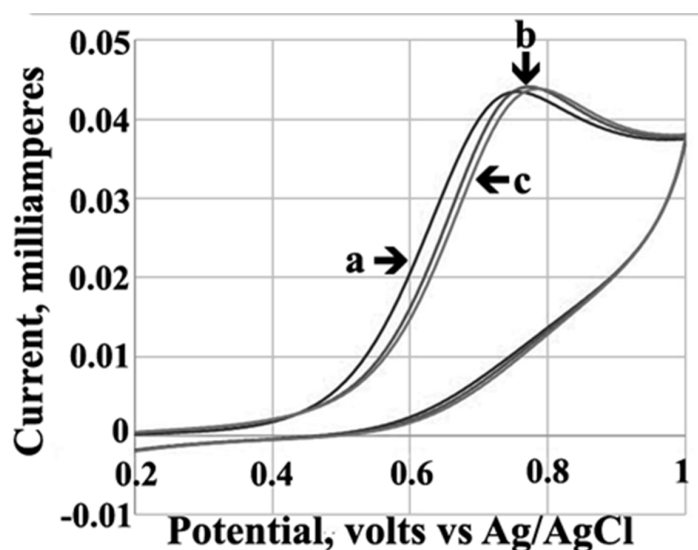
Figure 2 Cyclic voltammograms. Solution of 5 mM AV-153-K in 0.1 M Tris-HCl buffer (pH 7.4) without DNA (a) and in the presence of 10 µM (b) and 20 µM of DNA (c).

band intensity and decreased the positive band intensity. A 2 nm red shift of crossover point was also observed. These data clearly indicate interactions of the compound with DNA, although changes in spectra are not typical for any binding mode.

Interaction with bases

The above results indicate that the binding between AV-153-Na and DNA partly occurs via intercalation. The influences of DNA bases, C, G, A and T, on the UV/VIS absorption spectra of AV-153 were used to evaluate the possible base-specificity of binding (Fig. 4, Table 3). The absorption intensity gradually increased with an increase in the concentration of all the four bases. Affinity to G, C and T is greater than that to A. The results indicate that AV-153-Na can interact with the four types of bases, with somewhat different affinities. Titration was performed in solutions of 1M NaCl and 8M urea to evaluate the role of ionic and hydrogen bonds in AV-153-Na interactions with bases. During this process, the media affinity of AV-153-Na to bases was weakened, especially for G, and the shape of the spectra was also changed. However, interactions were not abolished.

FTIR spectroscopy of AV-153 salts and their complexes with DNA

The FTIR spectra of AV-153 salts showed several strong absorption bands (Fig. 5). In the spectra of all AV-153 salts, the most intensive were broad absorption bands with maximums in the wavenumber 1,220–1,243 cm^{-1} range, assigned to N-H bending and C-N stretching vibrations (*Zhang et al., 2013*), and 1,665–1,684 cm^{-1}, assigned to CO, C=O, C=N stretching vibrations (*Varsanyi, 1974*). The shape of the absorption bands in the wavenumber region of 1,570–1,670 cm^{-1} was quite different: (i) two sharp separate bands in spectra of AV-153 salt with K, Rb, Ca; (ii) two partly overlapping bands at 1,593 and 1,666 cm^{-1} in AV-153- Li; (iii) a broad strongly overlapping band with maximum at 1,684

Table 1 Affinity of the AV-153 salts to DNA determined by spectrofluorimetry and DNA binding parameters determined by cyclic voltammetry.

Compound	Protein binding constant	DNA binding constant, cyclic voltammetry	Number of electrons (n)	Number of binding sites DNA (s)	Number of binding sites protein
AV-153-Na	3.9×10^5				0.93
AV-153-Mg	4.3×10^5	3.44×10^4	0.52	4.87	0.93
AV-153-Ca	4.9×10^5	2.755×10^5	0.64	7.37	1.03
AV-153-K	5.2×10^5	2.28×10^4	0.71	2.60	1.12
AV-153-Li	1.08×10^6	7.20×10^4	0.54	5.60	2.25
AV-153-Rb	4.8×10^5	6.83×10^4	0.84	4.40	1.02

Table 2 The ability of the AV-153 salts to extrude the EtBr from intercalation sites.

Compound	K_{sv}, M^{-1}	Fluorescence decrease, % (+100 μM of compound)	Correlation coefficient
AV-153-Na	9.4×10^4	44	.99
AV-153-Ca	1.7×10^5	60	.99
AV-153-Mg	2.3×10^5	65	.99
AV-153-Li	9.9×10^4	50	.99
AV-153-K	8.7×10^4	42	.99
AV-153-Rb	8.9×10^4	45	.99

cm^{-1}. All the AV-153 salt spectra showed absorption bands at ∼1,025, ∼1,045, ∼1,101 and ∼1,128 cm^{-1}, with variable mutual intensities. The broad and strong absorption bands in the 900–1,200 cm^{-1} region were assigned to the stretching vibrations of C-O, C-C bonds and C-O, C-C, C-O-O deformation vibrations, though many other functional groups have bands in this region as well (*Naumann & Meyers, 2000*). Also, a separate strong absorption band in the 1,497–1,505 cm^{-1} region with slightly varying intensity (the lowest in AV-153-Rb) and the band at ∼1,498 cm^{-1} in spectra of Li, CA and Mg AV-153 salts while at 1,500 and 1,505 cm^{-1} in spectra of AV-153 salts with Rb and K correspondingly.

The evaluation of AV-153 salt spectral band intensities and shape showed major variations in the bands at ∼1,675 cm^{-1}, assigned to the C=O and/or C=C bonds and ∼1,234 cm^{-1}, assigned to the N-H and/or C-N bonds. These variations indicate the different metals binding with the AV-153.

The FTIR DNA spectrum was recorded to identify the specific absorption bands assigned to the DNA bases and PO_2^- groups. In the FTIR spectrum of sonicated ct-DNA (Fig. 6) we identified the specific absorption bands of DNA-bases: guanine (G) at 1,697 cm^{-1}, thymine (T) at 1,655 cm^{-1}, adenine (A) at 1,608 cm^{-1}, and cytosine (C) at 1,488 cm^{-1} (*Tajmir-Riahi, N'Soukpoé-Kossi & Joly, 2009*). The specific absorption bands of PO_2^- groups were detected at 1,241 cm^{-1} and assigned to the symmetric stretching vibrations, and at 1,093 cm^{-1}, which was assigned to the asymmetric stretching vibrations (*Banyay, Sarkar & Gräslund, 2003*; *Cherng, 2009*).
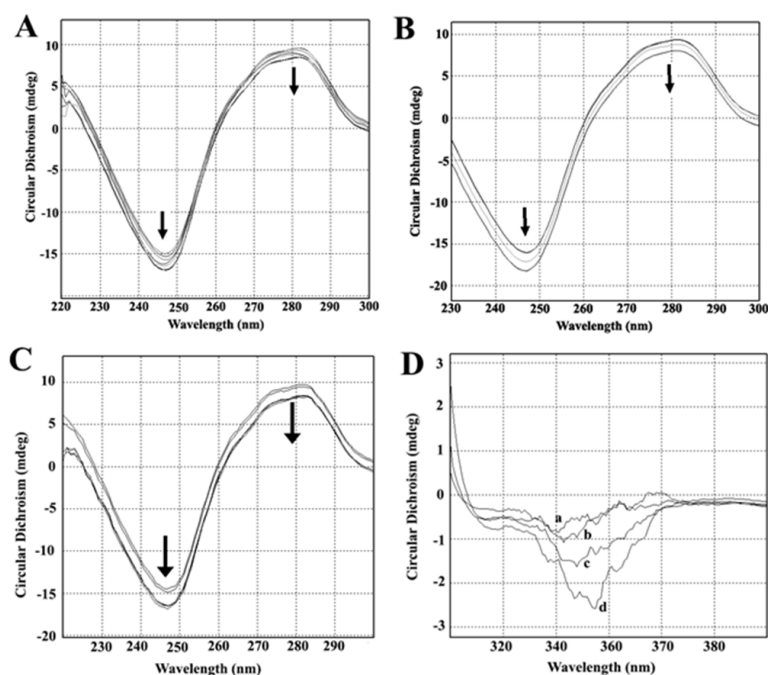
Figure 3 Circular dichroism experiments. Circular dichroism spectra of ct- DNA in absence and presence of (A) AV-153-Ca, (B) AV-153-Rb and (C) AV-153-Na. AV-153 salts concentration was increased by 10 μM at each step up to 40 μM. DNA concentration was 50 μM. Measurements were performed in 10 mM HEPES buffer. (D) Induced circular dichroism spectra of AV-153-Na (500 μM) in presence of 62.5 μM (A), 125 μM (B); 250 μM (C) and 500 μM (D) of DNA. Measurements were performed in HEPES buffer.

The comparison of DNA and DNA-AV-153 salt complexes spectra was used to identify the intensity and/or wavenumber shift changes that indicate the structural and conformational changes in DNA that is possibly related to interactions with AV-153 salts. The spectra of AV-153 salts mixed with DNA were vector normalized, and thus the intensity of the vibration bands is proportional to the concentration of particular bonds. The AV-153 salts spectra showed many intensive absorption bands (Fig. 5) but DNA-broad spectrum overlapped with absorption bands assigned to DNA-bases and two distinct PO_2^- group vibrations bands (Fig. 6). The profile of the AV-153 salt and DNA complex spectrum, being a superposition of both components, showed all specific DNA bands, but with variable intensities and band shapes compared to that of pure DNA (Fig. 7). Spectra cross-comparison was used to find the intensity and/or frequency changes assigned to structural changes in DNA caused by the binding with the AV-153 salt. In the DNA and salt complexes spectra, the position of a specific band of G at ~1,697 cm^{-1} was shifted to ~1,699 cm^{-1} by Li and K; ~1,693cm^{-1} by Mg; ~1,692 cm^{-1} by Rb and ~1,687 cm^{-1} by Ca. In the AV-153-Li and AV-153-K complex, the intensity of the G band decreased. The T band wavenumber (1,655 cm^{-1}) was shifted by Ca to 1,661 cm^{-1}, Rb to 1,653 cm^{-1} and Mg to 1,652 cm^{-1}. The intensity of specific T band was affected by all AV-153 salts but most of all by Ca and Mg salts. The A band wavenumber (~1,608 cm^{-1}) was slightly shifted
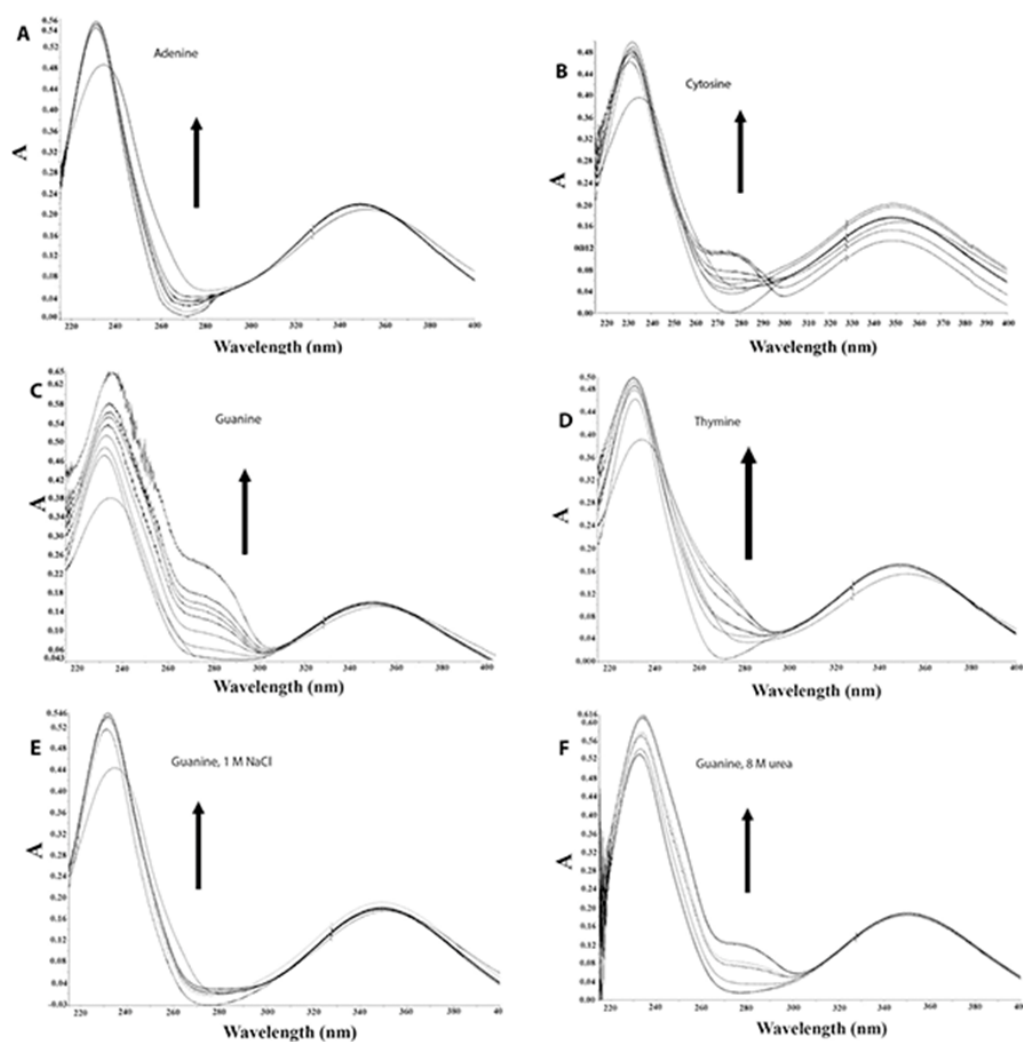
Figure 4 **AV-153-Na absorption spectra in absence and presence of bases in different solutions.** Concentrations of bases were increased for 10 μM with each titration. (A) Adenine, (B) Cytosine, (C, E, F) Guanine, (D) Thymine. (A–D) in 5 mM Tris HCl, pH 7.4, 50 mM NaCl; (E) 1 M NaCl; (F) 8 M urea.

to 1,606 cm^{-1} in the spectra of all the AV-153 salt complexes with DNA. The intensity was slightly increased by AV-153 salts of Ca, Mg and Rb. The C band intensity (1,488 cm^{-1}) was not affected by AV-153-Rb, but the other salts provoked an increase in intensity and no remarkable frequency shifts were detected. The intensity of the PO$_2$$^-$ groups at 1,241 cm^{-1} was significantly increased by AV-153-Ca salt only. AV-153-Li produced a frequency shift from 1,241 cm^{-1} to 1,238 cm^{-1} compared to that in the DNA spectrum. All salts modified the shaped and intensity of the bands assigned to PO$_2$$^-$ groups at 1,093 and 1,064 cm^{-1}. These PO$_2$$^-$ groups of DNA seem to be similarly affected by AV-153-K and -Li salts, showing two strongly overlapping bands and a decrease in intensities. Mg and Rb salts in complex with DNA significantly increased the band intensity at ∼1,065 cm^{-1} compared to that in the DNA spectrum. AV-153-Ca caused significant changes in the DNA, as a broad

Table 3 Affinity of the AV-153-Na to bases.

Base	Binding constants of the AV-153 salts in different media		
	AV-153-Na, 5 mM Tris–HCl, 50 mM NaCl	AV-153-Na, 1 M NaCl	AV-153-Na, 8 M urea
Adenine	2.9×10^3	2.3×10^3	2.5×10^3
Cytosine	3.6×10^3	2.8×10^3	3.0×10^3
Guanine	8.8×10^3	3.2×10^3	1.9×10^3
Thymine	3.5×10^3	5.11×10^3	3.1×10^3
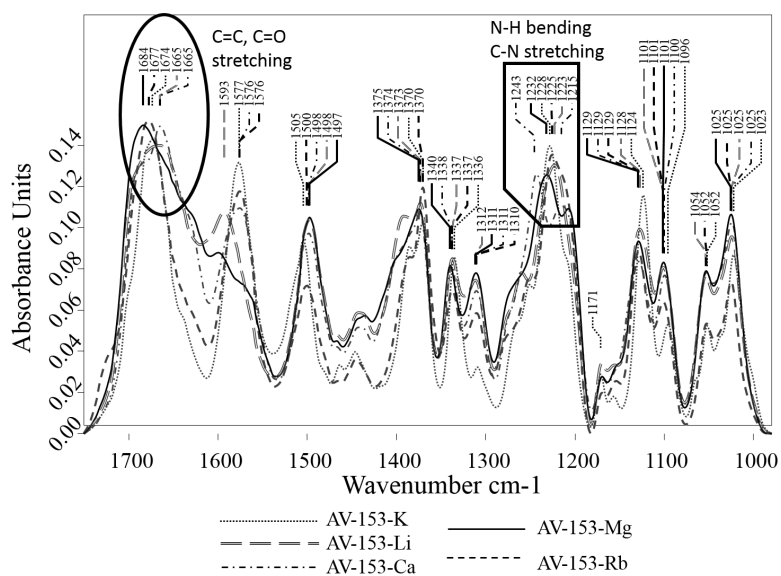
Figure 5 Vector normalized FTIR spectra of AV-153 salts. Major variations of C=O/C=C and N-H/C-N bands at ~1,675 and ~1,234 cm^{-1}, respectively are shown.

strongly overlapping band with maximums at ~1,097 and ~1,093 cm^{-1} in DNA spectra was split into two distinct bands in AV-153-Ca spectra and DNA complexes.

The second derivative spectra of AV-153 salts, DNA and their complexes were used to evaluate the binding of AV-153 salts with A, T, C or G. The second derivative spectra of DNA complexes with AV-153-K and AV-153-Li showed (i) significant increase of G and C absorption band intensities, (ii) a shift of T absorption band maximum from 1,649 cm^{-1} to 1,654/55 cm^{-1}, (iii) a band was not significantly changed (Fig. 8A). The second derivative spectra of DNA complexes with AV-153-Ca, AV-153-Mg and AV-153-Rb showed (i) an increase in G and a decrease in C band intensities, (ii) the intensities of A and T bands were unaffected, (iii) a shift in the peak assigned to C with a maximum range of 1,489 to 1,494/95 cm^{-1} (Fig. 8B).
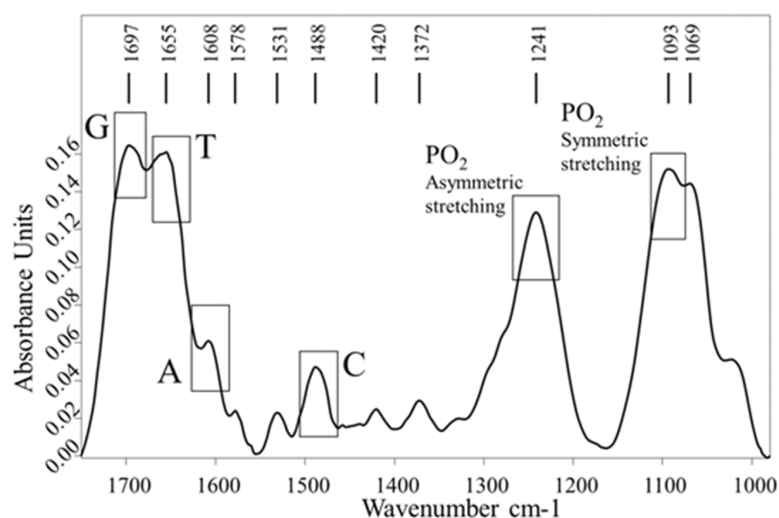
Figure 6 FTIR spectra of the ct-DNA. Absorptions of DNA bases (Adenine –A, Guanine –G, Cytosine – C, Thymine –T) and PO$_2$ groups are marked.
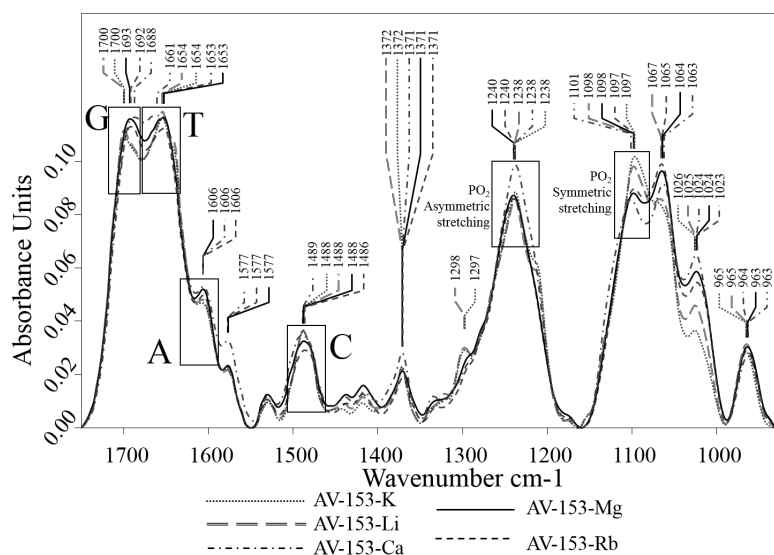
Figure 7 Vector normalized FTIR spectra of DNA mixed with AV-153 salts in ratio of 5:1. Wavenumber shifts and/or absorption intensity changes in all bands assigned to DNA bases are shown.

Interaction with guanine quadruplexes

Incubation of the human telomere repeat oligonucleotide with 100 mM NaCl resulted in the formation of G4. The CD spectroscopy revealed a dominating band at 295 nm and a shallow negative band around 260 nm. Such CD spectra correspond to the two-tetrad, chair type G4. Salts from monovalent metals were tested for interaction with G4. The titration of the G4 with AV-153-Na made the peaks more pronounced (Fig. 9A), as did AV-153-K (Fig. 9B). AV-153-Li made the negative peak deeper, but the intensity of the
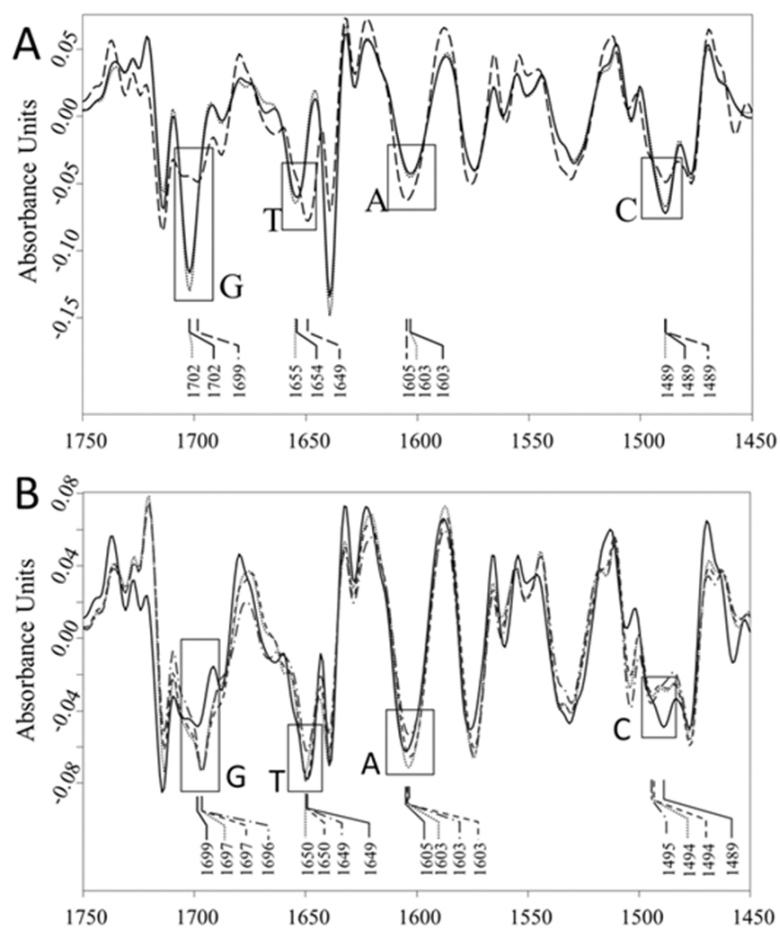
Figure 8 Vector normalized FTIR spectra. (A) Vector normalized second derivative spectra of the ct-DNA (solid line), dotted line –DNA with AV-153-Li (5:1), and dashed line –DNA with AV-153-K (5:1); (B) Vector normalized second derivative spectra of the ct-DNA (solid line), dotted line –DNA with AV-153-Mg (5:1), dash dotted line –DNA with AV-153-Ca (5:1), and dashed line –DNA with AV-153-Rb (5:1).

positive peak decreased (Fig. 9C), while the AV-153-Rb did not induce any changes in the CD spectra (Fig. 9D).

Affinity to G4 and single-strand oligos was further tested using UV.VIS spectroscopy. Changes in the AV-153-Na spectra upon addition of G4 or single-strand oligonucleotides are presented in Fig. 10. Hypochromic and slight bathochromic effects are observed. Affinity to G4 is higher than to single-stranded DNA. Other salts produced similar changes in spectra (not shown), and the binding constants are given in Table 4. AV-153-Na and AV-153-K manifested higher affinity to G4, and AV-153-Li and AV-153-Rb to single-stranded DNA.

DISCUSSION

Metal ions modify the affinity to DNA of coordination complexes formed by organic compounds. For example, 2-[2-bromoethyliminomethyl]-4-[ethoxymethyl]phenol
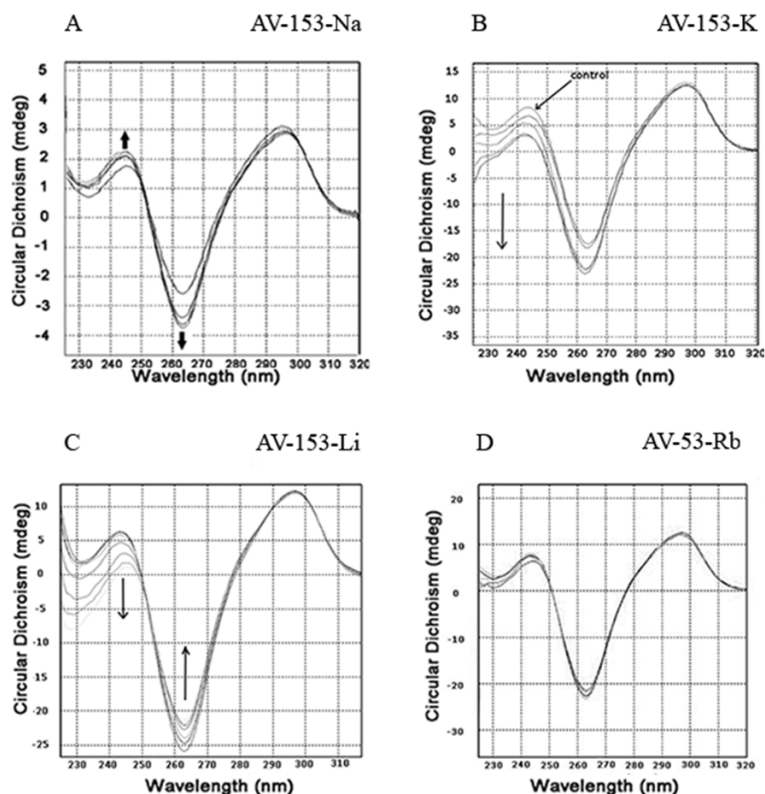
Figure 9 Circular dichroism spectra of the human telomere repeat oligonucleotide. Spectra were taken before and after adding of the monovalent AV-153 salts in increasing concentrations: 5 μM of the oligonucleotide were titrated in 10 mM sodium phosphate buffer, 0.3 mM EDTA, 100 mM NaCl, pH 7.2 with 10 μM of AV-153 salt at each step. (A) AV-153-Na; (B) AV-153-K; (C) AV-153-Li; (D) AV-153-Rb.

derivative Zn-derivative manifests a higher binding constant than copper and nickel derivatives (*Lee et al., 2016*). Similarly, 6-methyl-3-formyl chromone-derived hydrazine complexes with Ni have a higher binding constant to DNA than Zn and Cu complexes (*Philip et al., 2017*). Zn and Co phthalocyanine complexes bind to DNA in different ways; the former is an intercalator and the latter a groove binder (*Özen, Günel & Baran, 2018*). However, in coordination complexes, the metal does not dissociate from the organic moiety in the solution. The differences in the DNA-binding affinity of AV-153 salts revealed in this study might seem surprising if one assumes that salts should be completely dissociated in solution. However, metal ions and carbonic acid are in equilibrium during association and dissociation (*Koczoń et al., 2005*). All the solution measurements were performed at neutral pH, where AV-153 salts are ionized as pKs of the salts ranged between pH 4.24 and 4.52 (*Leonova et al., 2019*). The FTIR spectra of the compounds clearly indicate profound differences in structure also of the non-ionized forms of the salts. These might be responsible for the different effects of the compounds.

During the cyclic voltammetry experiments, the direct interaction of the compounds with DNA caused a shift in the peak potential. This reproduced the results obtained by UV/VIS spectroscopy and spectrofluorimetry (*Buraka et al., 2014*; *Leonova et al., 2019*).
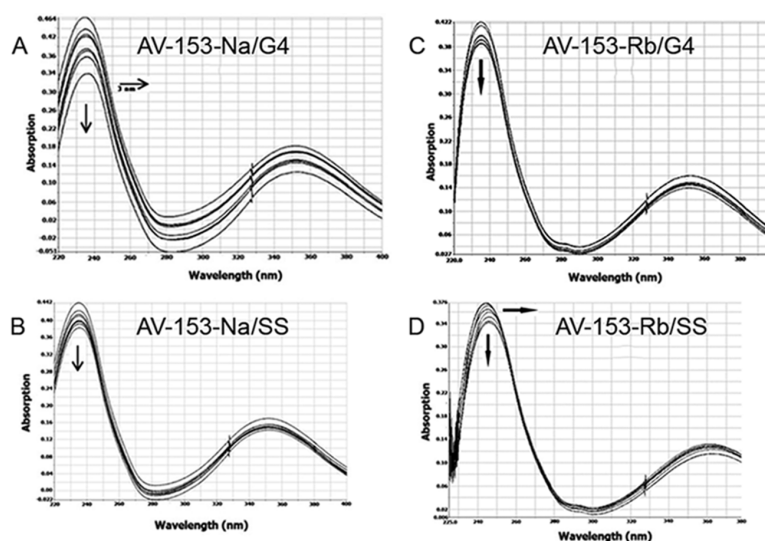
Figure 10 **Absorption spectra of 25 μM AV-153-Na (A, B) and AV-153-Rb (C, D) in absence and presence of guanine G4 (A, C) and single-stranded (SS) human telomeric repeat (B, D).** Titration was performed in 10 mM sodium phosphate buffer, 0.3 mM EDTA, 100 mM NaCl, pH 7.2, 50 nM of oligonucleotide were added each time.

Moreover, these results indicate the intercalation of the compound to DNA double-helix (*Sirajuddin, Ali & Badshah, 2013*). We did not observe a decrease in the peak current, which is considered the main consequence of drug-DNA complex formation (*Sirajuddin, Ali & Badshah, 2013*). We also observed a significant increase in the peak current during the formation of the complex between DNA and terbium(III)-deferasirox (*Shaghaghi et al., 2014*) or 3,4-disubstituted 1,8-naphthalimide (*Sharma et al., 2019*). Thus, the increase in peak current, which is slight in the case of AV-153 salts, can be interpreted as a consequence of DNA and drug interaction. The ability of AV-153 salts to intercalate DNA molecule (at least partly) was confirmed by EtBr displacement assay and circular dichroism spectroscopy. The presence of a negative induced circular dichroism band, increasing with every added DNA portion with a red shift, again indicates an intercalative binding mode (*Garbett, Ragazzon & Chaires, 2007*; *Thimmaiah et al., 2015*). Interestingly, a recent study of the DNA-binding of 1,4-DHP with Ca channel blocker activity, performed mostly by electrochemical methods, also revealed an interaction of the compounds with DNA, although with much lower affinity compared to the AV-153 salts (*Shahzad et al., 2019*). We also compared the ability of AV-153 salts to interact with the human telomeric G4 repeat and single-stranded DNA. The presence of the affinity of some salts to the G4 opens a window for the assessment of the pharmacological properties of AV-153 salts in human telomeric-related abnormalities, while the differences in affinities show the important role of salt-forming metal ions on the molecular effect of the salts.

Cross-comparison FTIR spectra of AV-153 salts showed differences in spectrum profiles and band intensities, which reflect the differences in IR-active bonds. Although AV-153 salts spectra showed several absorption bands with similar profiles and intensities, no

Table 4 Binding constants of the AV-153 salts with G4 forming and single-stranded human telomeric repeat.

Compound	Kb (M^{-1}) G4	Kb (M^{-1}) single-stranded
AV-153-Na	1.04×10^6	4.49×10^5
AV-153-K	4.18×10^5	1.90×10^5
AV-153-Li	2.23×10^5	2.61×10^5
AV-153-Rb	2.09×10^5	2.84×10^5

identical absorption bands were detected. Thus, it can be assumed that Ca, K, Mg, Li ions and Rb affect all IR-sensitive AV-153 bonds.

The FTIR spectrum of a multicomponent mixture is a result of the overlapping spectra of each constituent element. The absorption band intensity changes and/or wavenumber shifts could point to the interactions between constituents, particularly assigned to bonds specific to AV-153 salt and DNA complex. The FTIR spectra of AV-153 salts showed many strong absorption bands, evidence of their interactions with DNA, particularly with DNA-bases and PO_2^- groups, should be different. After summarizing the results of FTIR spectroscopy, we concluded that: (i) the G band maximum was shifted and the intensity decreased by AV-153-K, Li and Ca salts (ii) all salts increased the intensity of T band, (iii) only AV-153-Rb did not affect the C-band, (iv) the intensity of PO_2^- band at 1,241 cm^{-1}, (iv) all salts changed the profile and mutual ratio of PO_2^- bands at 1,097 and 1,064 cm^{-1}. The FTIR spectra showed that DNA is less affected by AV-153-Rb but most of all by AV-153-Mg and AV-153-Ca.

Nafisi et al. (2008), *Nafisi, Montazeri & Manouchehri (2012)* and *Saito et al. (2012)* posit that the increase in absorption band intensities point to the partial helix destabilization of DNA, while a decrease in absorption band intensities indicate DNA stabilization, substance interaction, and conformational DNA changes.

The deconvolution (second derivative) of spectral bands is an approach for more precise evaluation of weak intensity and/or broad overlapping spectral bands. In deconvoluted spectra of DNA complexes with AV-153-K and AV-153-Li, we detected similar changes in spectral bands assigned to G, C, and T. In the spectra of the DNA complex with AV-153-Ca and AV-153-Rb, the bands assigned to G and C were modified, unlike pure DNA. The spectrum of the DNA complex with AV-153-Mg showed modifications of G, A, and C bands. The results of the FTIR spectroscopy showed the binding of AV-153 salts with DNA by structural and conformational changes of bonds assigned to DNA-bases and phosphate groups. Significant changes to the absorption bands assigned to the symmetric PO_2^- group, stretching vibrations at ~1,093 and ~1,064 cm^{-1}, indicate either conformational changes to the DNA molecule – form B changing to form A or Z, or partial denaturation of the molecule (*Whelan et al., 2011*; *Wood, 2016*). The characteristic IR-bands of G and C were more affected by the AV-153 salt than those of T and A. Consequently, G and C possess a higher potential to attach/bind the AV-153 salts. A UV/VIS spectroscopy of AV-153-Na complexes with bases also revealed a higher affinity to G band. The increased affinity of some AV-153 salts to the G band, revealed by the UV/VIS spectroscopy, was confirmed by FTIR spectroscopy which showed that native AV-153 salts also preferably interacted with G.

The interaction with bases again indicates the possibility of an intercalative DNA-binding mode for AV-153 salts. However, interactions with phosphate groups and the different efficiency of the EtBr extrusion for different salts indicate the possibility of alternative ways of interaction, such as groove binding. The possibility of different modes of interaction with DNA was confirmed in experiments with G4 and single-stranded oligonucleotides. Hypochromic effects were observed during these experiments on the interaction of these compounds with native DNA (*Buraka et al., 2014*) and bases. Metal atoms again modified affinity to different oligonucleotides conformation, as some salts had a higher affinity to G4, and others to single-stranded DNA.

This study has limitations that we intend to overcome in subsequent research. The limitations concern both the methods applied and the chosen objects. NMR experiments should be performed using oligonucleotides-forming double-stranded, single-stranded, nicked- and G4-forming DNA. These oligonucleotides should be used for FTIR experiments. We also could not use acridine orange and Hoechst dyes for spectrofluorometric measurements due to the overlap of the emission spectra of these dyes with the emission spectrum of the AV-153. We hope dyes with different spectra will become available soon.

CONCLUSION

Metal ions modify the affinity of AV-153 salts to DNA, DNA bases and G4 and the interaction mode between DNA and AV-153.

ACKNOWLEDGEMENTS

We thank U Kalnenieks and R Rutkis (Institute of Microbiology and Biotechnology at the University of Latvia) for giving us access to their equipment.

Funding

The work was supported from the grant of the Latvian Council of Science and an inner grant of the Latvian Institute of Organic Synthesis. The funders had no role in study design, data collection and analysis, decision to publish, or preparation of the manuscript.

Grant Disclosures

The following grant information was disclosed by the authors:
Latvian Council of Science.
Latvian Institute of Organic Synthesis.

Competing Interests

Nikolajs Sjakste is an Academic Editor for PeerJ.

Author Contributions

- Elina Leonova, Karlis Shvirksts and Edgars Smelovs conceived and designed the experiments, performed the experiments, analyzed the data, prepared figures and/or tables, and approved the final draft.
- Vitalijs Borisovs conceived and designed the experiments, performed the experiments, prepared figures and/or tables, and approved the final draft.
- Jelizaveta Sokolovska conceived and designed the experiments, performed the experiments, analyzed the data, prepared figures and/or tables, authored or reviewed drafts of the paper, and approved the final draft.
- Egils Bisenieks, Gunars Duburs and Nikolajs Sjakste conceived and designed the experiments, prepared figures and/or tables, authored or reviewed drafts of the paper, and approved the final draft.
- Mara Grube conceived and designed the experiments, authored or reviewed drafts of the paper, and approved the final draft.

Data Availability

The raw measurements are presented in Supplemental Files.

Supplemental Information

Supplemental information for this article can be found online at http://dx.doi.org/10.7717/peerj.10061#supplemental-information.

REFERENCES

Aghaei R, Mazloum-Ardakani M, Abdollahi-Alibeik M, Moshtaghioun SM, Rezaeipoor-Anari A, Haghighijoo Z, Zamani L. 2017. A new electrochemical biosensor based on telomeric G-quadruplex DNA: In silico and experimental study of dihydropyridine derivatives potential effect on telomerase inhibition. *Journal of Electroanalytical Chemistry* **796**:24–32 DOI 10.1016/j.jelechem.2017.04.055.

Aslanoglu M. 2006. Electrochemical and spectroscopic studies of the interaction of proflavine with DNA. *Analytical Sciences* **22(3)**:439–443 DOI 10.2116/analsci.22.439.

Augustyniak A, Bartosz G, Cipak A, Duburs G, HorákováL Luczaj W, Majekova M, Odysseos AD, Rackova L, Skrzydlewska E, Stefek , Strosová M, Tirzitis G, Venskutonis PR, Viskupicova J, Panagiota PS, Zarković N. 2010. Natural and synthetic antioxidants: an updated overview. *Free Radical Research* **44(10)**:1216–1262 DOI 10.3109/10715762.2010.508495.

Banyay M, Sarkar M, Gräslund A. 2003. A library of IR bands of nucleic acids in solution. *Biophysical Chemistry* **104(2)**:477–488 DOI 10.1016/S0301-4622(03)00035-8.

Buraka E, Chen CY, Gavare M, Grube M, Makarenkova G, Nikolajeva V, Bisenieks I, Brūvere I, Bisenieks E, Duburs G, Sjakste N. 2014. DNA-binding studies of AV-153, an antimutagenic and DNA repair-stimulating derivative of 1,4-dihydropiridine. *Chemico-Biological Interactions* **220**:200–207 DOI 10.1016/j.cbi.2014.06.027.

Cherng JY. 2009. Investigation of DNA spectral conformational changes and polymer buffering capacity in relation to transfection efficiency of DNA/polymer complexes. *Journal of Pharmacy & Pharmaceutical Sciences* **12(3)**:346–356 DOI 10.18433/J3859K.

Dišlere K. 2019. The effect of 1,4-dihydropyridine derivatives on expression of DNA repair and proteolysis enzymes in diabetes mellitus and on the level of double-strand DNA breaks in vitro. Summary of doctoral thesis, University of Latvia, Riga.

Duburs G, Uldrikis J. 1969. Preparation of 2,6-dimethyl-3,5-bis(ethoxycarbonyl)-1,4-dihydroisonicotinic acid and their salts. *Khimiya Geterotsiklicheskikh Soedinenii* **6**:1015–1017.

Feng Q, Li N-Q, Jiang Y-Y. 1997. Electrochemical studies of porphyrin interacting with DNA and determination of DNA. *Analytica Chimica Acta* **344(1)**:97–104 DOI 10.1016/S0003-2670(97)00008-1.

Garbett NC, Ragazzon PA, Chaires JB. 2007. Circular dichroism to determine binding mode and affinity of ligand-DNA interactions. *Nature Protocols* **2(12)**:3166–3172 DOI 10.1038/nprot.2007.475.

Geall AJ, Blagbrough IS. 2000. Rapid and sensitive ethidium bromide fluorescence quenching assay of polyamine conjugate-DNA interactions for the analysis of lipoplex formation in gene therapy. *Journal of Pharmaceutical and Biomedical Analysis* **22(5)**:849–859 DOI 10.1016/S0731-7085(00)00250-8.

Geethanjali HS, Nagaraja D, Melavanki RM, Kusanur RA. 2015. Fluorescence quenching of boronic acid derivatives by aniline in alcohols –a negative deviation from Stern–Volmer equation. *Journal of Luminescence* **167**:216–221 DOI 10.1016/j.jlumin.2015.06.040.

Ghosh R, Bhowmik S, Bagchi A, Das D, Ghosh S. 2010. Chemotherapeutic potential of 9-phenyl acridine: biophysical studies on its binding to DNA. *European Biophysics Journal* **39(8)**:1243–1249 DOI 10.1007/s00249-010-0577-z.

Gong AQ, Zhu XS. 2013. Determination of epristeride by its quenching effect on the fluorescence of L-tryptophan. *Journal of Pharmaceutical Analysis* **3(6)**:415–420 DOI 10.1016/j.jpha.2013.05.001.

Koczoń P, Piekut J, Borawska M, Swisłocka R, Lewandowski W. 2005. The relationship between chemical structure and antimicrobial activity of selected nicotinates, p-iodobenzoates, picolinates and isonicotinates. *Spectrochimica Acta Part A Molecular and Biomolecular Spectroscopy* **61(8)**:1917–1922 DOI 10.1016/j.saa.2004.07.022.

Lee YS, Doonan BB, Wu JM, Hsieh TC. 2016. Combined metformin and resveratrol confers protection against UVC-induced DNA damage in A549 lung cancer cells via modulation of cell cycle checkpoints and DNA repair. *Oncology Reports* **35(6)**:3735–3741 DOI 10.3892/or.2016.4740.

Leonova E, Ošiņa K, Duburs G, Bisenieks E, Germini D, Vassetzky Y, N. Sjakste. 2019. Metal ions modify DNA-protecting and mutagen-scavenging capacities of the AV-153 1,4-dihydropyridine. *Mutation Research/Genetic Toxicology and Environmental Mutagenesis* **845**:Article 403077 DOI 10.1016/j.mrgentox.2019.06.007 .
Leonova E, Rostoka E, Sauvaigo S, Baumane L, Selga T, Sjakste N. 2018. Study of interaction of antimutagenic 1,4-dihydropyridine AV-153-Na with DNA-damaging molecules and its impact on DNA repair activity. *PeerJ* **6**:e4609 DOI 10.7717/peerj.4609.

Lewandowski W, Kalinowska M, Lewandowska H. 2005. The influence of metals on the electronic system of biologically important ligands. Spectroscopic study of benzoates, salicylates, nicotinates and isoorotates. Review. *Journal of Inorganic Biochemistry* **99(7)**:1407–1423 DOI 10.1016/j.jinorgbio.2005.04.010.

Milkovic L, Vukovic T, Zarkovic N, Tatzber F, Bisenieks E, Kalme Z, Bruvere I, Ogle Z, Poikans J, Velena A, Duburs G. 2018. Antioxidative 1, 4-dihydropyridine derivatives modulate oxidative stress and growth of human osteoblast-like cells in vitro. *Antioxidants* **7(9)**:123 DOI 10.3390/antiox7090123.

Nafisi S, Manouchehri F, Tajmir-Riahi H-A, Varavipour M. 2008. Structural features of DNA interaction with caffeine and theophylline. *Journal of Molecular Structure* **875(1–3)**:392–399 DOI 10.1016/j.molstruc.2007.05.010.

Nafisi S, Montazeri M, Manouchehri F. 2012. The effect of Se salts on DNA structure. *Journal of Photochemistry and Photobiology. B, Biology* **113**:36–41 DOI 10.1016/j.jphotobiol.2012.04.012.

Naumann D, Meyers R. 2000. *Encyclopedia of analytical chemistry.* Chichester: John Wiley & Sons, 102–131.

Özen F, Günel A, Baran A. 2018. DNA-binding, enzyme inhibition, and photochemical properties of chalcone-containing metallophthalocyanine compounds. *Bioorganic Chemistry* **81**:71–78 DOI 10.1016/j.bioorg.2018.08.002.

Philip JE, Shahid M, Prathapachandra Kurup MR, Velayudhan MP. 2017. Metal based biologically active compounds: design, synthesis, DNA binding and antidiabetic activity of 6-methyl-3-formyl chromone derived hydrazones and their metal (II) complexes. *Journal of Photochemistry and Photobiology. B, Biology* **175**:178–191 DOI 10.1016/j.jphotobiol.2017.09.003.

Ryabokon NI, Goncharova RI, Duburs G, Hancock R, Rzeszowska-Wolny J. 2008. Changes in poly(ADP-ribose) level modulate the kinetics of DNA strand break rejoining. *Mutation Research/DNA Repair* **637(1–2)**:173–181.

Ryabokon NI, Goncharova RI, Duburs G, Rzeszowska-Wolny JA. 2005. 1,4-dihydropyridine derivative reduces DNA damage and stimulates DNA repair in human cells in vitro. *Mutation Research/DNA Repair* **587(1–2)**:52–58.

Ryabokon NI, Nikitchenko NV, Dalivelya OV, Goncharova RI, Duburs G, Konopacka M, Rzeszowska-Wolny J. 2009. Modulation of cellular defense processes in human lymphocytes in vitro by a 1,4-dihydropyridine derivative. *Mutation Research/DNA Repair* **679(1–2)**:33–38.

Saito ST, Silva G, Pungartnik C, Brendel M. 2012. Study of DNA-emodin interaction by FTIR and UV-vis spectroscopy. *Journal of Photochemistry and Photobiology. B, Biology* **111**:59–63 DOI 10.1016/j.jphotobiol.2012.03.012.

Shaghaghi M, Dehghan G, Jouyban A, Sistani P, Arvin M. 2014. Studies of inter-action between terbium(III)-deferasirox and double helix DNA by spectral and

electrochemical methods. *Spectrochimica Acta Part A Molecular and Biomolecular Spectroscopy* **120**:467–472 DOI 10.1016/j.saa.2013.09.073.

Shahzad S, Dogan-Topal B, Karadurmus L, Caglayan MG, Taskin Tok T, Uslu B, Shah A, Ozkan SA. 2019. Electrochemical, spectroscopic and molecular docking studies on the interaction of calcium channel blockers with dsDNA. *Bioelectrochemistry* **127**:12–20 DOI 10.1016/j.bioelechem.2018.12.007.

Sharma H, Sidhu JS, Hassen WM, Singh N, Dubowski JJ. 2019. Synthesis of a 3, 4-disubstituted 1, 8-naphthalimide-based DNA intercalator for direct imaging of *Legionella pneumophila*. *ACS Omega* **4(3)**:5829–5838 DOI 10.1021/acsomega.8b03638.

Sirajuddin M, Ali S, Badshah A. 2013. Drug-DNA interactions and their study by UV-Visible, fluorescence spectroscopies and cyclic voltametry. *Journal of Photochemistry and Photobiology. B, Biology* **124**:1–19 DOI 10.1016/j.jphotobiol.2013.03.013.

Tajmir-Riahi HA, N'Soukpoé-Kossi CN, Joly D. 2009. Structural analysis of protein–DNA and protein–RNA interactions by FTIR, UV-visible and CD spectroscopic methods. *Journal of Spectroscopy* **23**:Article 587956 DOI 10.3233/SPE-2009-0371.

Thimmaiah K, Ugarkar AG, Martis EF, Shaikh MS, Coutinho EC, Yergeri MC. 2015. Drug-DNA interaction studies of acridone-based derivatives. *Nucleosides Nucleotides Nucleic Acids* **34(5)**:309–331 DOI 10.1080/15257770.2014.992531.

Varsanyi G. 1974. *Assignments for vibrational spectra of seven hundred benzene derivatives.* New York: Wiley.

Wahba MEK, El-Enany N, Belal F. 2015. Application of the Stern–Volmer equation for studying the spectrofluorimetric quenching reaction of eosin with clindamycin hydrochloride in its pure form and pharmaceutical preparations. *Analytical Methods* **7(24)**:10445–10451 DOI 10.1039/C3AY42093K.

Wang Q, Wang X, Zhanglong Z, Yuan X, Jiao K. 2011. Spectroscopic and electrochemical studies on the binding mechanism of DNA with an anthraquinone biological dye, nuclear fast red. *International Journal of Electrochemical Science* **6**:5470–5548.

Whelan DR, Bambery KR, Heraud P, Tobin MJ, Diem M, McNaughton D, Wood BR. 2011. Monitoring the reversible B to A-like transition of DNA in eukaryotic cells using Fourier transform infrared spectroscopy. *Nucleic Acids Research* **39(13)**:5439–5448 DOI 10.1093/nar/gkr175.

Wood BR. 2016. The importance of hydration and DNA conformation in interpreting infrared spectra of cells and tissues. *Chemical Society Reviews* **45(7)**:1980–1998 DOI 10.1039/C5CS00511F.

Zhang ZP, Rong MZ, Zhang MQ, Yuan C. 2013. Alkoxyamine with reduced homolysis temperature and its application in repeated autonomous self-healing of stiff polymers. *Polymer Chemistry* **4(17)**:4648–4654 DOI 10.1039/c3py00679d.